Properties of ^{37}Ar. I. Levels below 3.8 MeV (populated in ^{34}S(α,nγ)^{37}Ar)

1974 J. Phys. A: Math. Nucl. Gen. 7 83

(http://iopscience.iop.org/0301-0015/7/1/016)

J. Phys. A: Math., Nucl. Gen., Vol. 7, No. 1, 1974. Printed in Great Britain.

Properties of ^{37}Ar (I): levels below 3·8 MeV

L L Gadeken, P J Nolan, P A Butler, L L Green, A N James, J F Sharpey-Schafer and D A Viggars

Oliver Lodge Laboratory, University of Liverpool, PO Box 147, Liverpool L69 3BX, UK

Received 14 June 1973

Abstract. Excitation energies, mean lifetimes, γ-ray branching ratios, angular correlations, mixing ratios, and linear polarizations have been measured for the first twelve levels of ^{37}Ar using the ^{34}S$(\alpha, n\gamma)^{37}$Ar reaction. Parity assignments were made for the following levels: 3173 keV, $\frac{5}{2}^+$, 3274 keV, $\frac{5}{2}^-$, 3527 keV, $\frac{7}{2}^-$, and 3602 keV, $\frac{3}{2}^+$ or $\frac{5}{2}^-$. The spin and parity of the 3707 keV state ($\tau_m = 370 \pm 95$ fs) was determined, $J^\pi = \frac{11}{2}^-$. Three new low energy γ-ray transitions were observed and six new mixing ratios were determined. We find that the negative parity levels which decay to the 1611 keV $\frac{7}{2}^-$ state are represented qualitatively by the core excitation model.

1. Introduction

We have investigated the properties of the low-lying levels of ^{37}Ar as part of a systematic study of negative parity levels in s–d shell nuclei. Gamma transitions in ^{37}Ar have recently been the subject of much study. The reactions used and the corresponding references are listed below: ^{37}Cl(p, nγ)^{37}Ar (Kruzek *et al* 1973, Luketina *et al* 1972, Wong *et al* 1972, Taras *et al* 1971, Randolph *et al* 1971, Caraca *et al* 1971); ^{36}Ar(n, γ)^{37}Ar (Hardell and Beer 1970, Wille 1968, Skeppstedt *et al* 1968); ^{36}Ar(d, pγ)^{37}Ar (Champlin *et al* 1971); ^{35}Cl$(\tau, p\gamma)^{37}$Ar (Ivascu *et al* 1971); ^{34}S$(\alpha, n\gamma)^{37}$Ar (Verucchi *et al* 1973, Taras *et al* 1972, Ragan *et al* 1971a, b, Alenius *et al* 1972). Particle experiments using the ^{36}Ar(d, p)^{37}Ar reaction have been performed by Mermaz *et al* (1971) and Sen *et al* (1971). A summary of the experimental studies reported prior to 1968 may be found in Endt and van der Leun (1967). These investigations did not produce a clear picture of the level structure of ^{37}Ar. We will show below that the negative parity levels of this nucleus may be explained as an $f_{7/2}$ neutron coupled to a vibrational ^{36}Ar core.

The energy level diagram is shown in figure 1. The energies of the levels and the γ rays as well as all the branching ratios except two are values obtained in this work. The spin and parity assignments are a synthesis of present and previous results.

2. Experimental method

The states in ^{37}Ar were populated by the ^{34}S$(\alpha, n\gamma)^{37}$Ar reaction ($Q = -4{\cdot}629$ MeV) at bombarding energies of 9·0 MeV, 9·5 MeV, and 11·5 MeV. The targets were cadmium sulphide; the sulphur content was enriched to 90% ^{34}S. For all measurements the γ ray

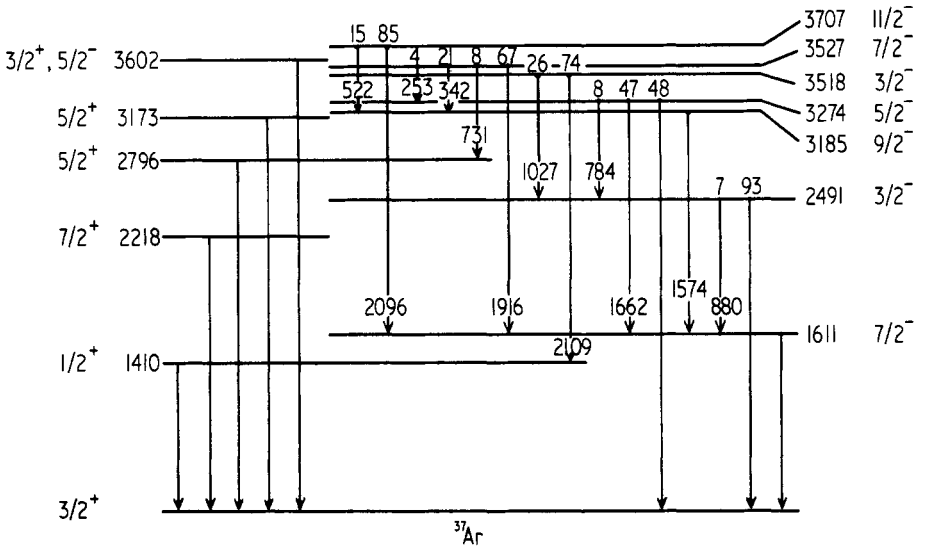

Figure 1. Energy level and decay scheme for the first twelve excited states of ^{37}Ar. The energies of the levels and the gamma transitions have been rounded to the nearest keV. Precise energies are given in table 1. The relative intensities (%) are shown and given with the associated errors in table 5.

detectors were calibrated for energy and efficiency by using the known γ ray energies and relative intensities of a ^{56}Co source (Camp and Meredith 1971).

The targets for the Döppler shift attenuation method (DSAM) mean lifetime, angular distribution, and linear polarization measurements consisted of approximately 1·0 mg cm^{-2} CdS which had been evaporated onto a thick gold backing. The gamma radiation was detected by an escape-suppressed and pair-escape spectrometer (Sharpey-Schafer *et al* 1971) which was positioned so that the central Ge(Li) detector was 24 cm from the target. At 1332 keV this detector had a resolution of 2·4 keV and a relative efficiency of 9%. A typical γ ray spectrum is shown in figure 2. The gamma linear polarizations were measured for a beam energy of 9·5 MeV using the three Ge(Li) Compton polarimeter described by Butler *et al* (1973).

The mean lifetime of the long-lived 1611 keV state was measured by the recoil distance method (RDM). The apparatus and data analysis are described by Nolan *et al* (1973) and references therein. The target was composed of 40 μg cm^{-2} CdS deposited upon 2·3 mg cm^{-2} nickel backing.

A gamma–gamma coincidence experiment was performed at a bombarding energy of 11·5 MeV in order to clarify the decay scheme of ^{37}Ar below an excitation energy of 5·5 MeV. The target chamber was a thin-walled stainless steel tube of 3·8 cm diameter. The self-supporting CdS target was about 200 μg cm^{-2} thick and was mounted 20 cm in front of a gold beam stop. Two Ge(Li) detectors were located 4 cm from the target at an angle of 90° relative to the beam direction and to each other. The vertical and horizontal detectors had resolutions of 4·0 keV and 3·0 keV respectively for 1332 keV gamma radiation. Sufficient lead shielding was used so that a negligible number of γ rays from the beam stop reached the detectors and so that scattered γ rays from either detector were severely attenuated before arriving at the other detector.

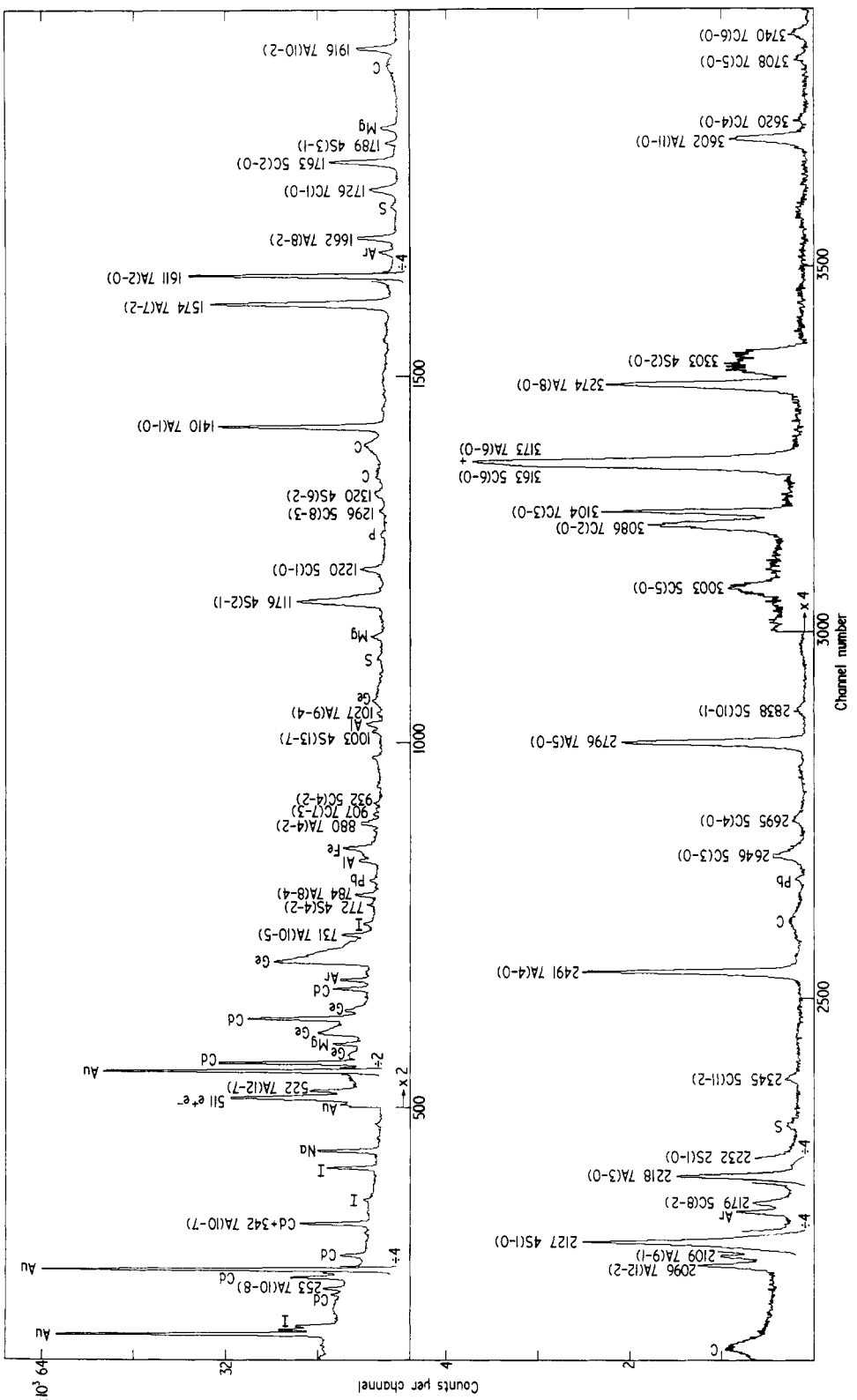

Figure 2. Escape-suppressed spectrum obtained at an angle of 90° for 9·5 MeV alphas incident on $Cd^{34}S$. Peaks due to transitions in the nuclei, ^{37}Ar, ^{37}Cl, ^{35}Cl, ^{34}S, and ^{32}S are labelled 7A, 7C, 5C, 4S, and 2S, respectively. The letters C, D, and S indicate Compton edges and double and single escape peaks. The contaminant peaks are identified by the appropriate symbols.

3. Results

3.1. DSAM lifetimes

The centroids of peaks due to all the observed γ rays except the 2109 keV transition were extracted from data obtained at bombarding energies of 9·0 MeV and 9·5 MeV for seven angles, 125°, 110°, 90°, 60°, 45°, 30° and 0°. The gain and zero energy of the system were monitored using peaks in the γ-ray spectra which were known to have energies independent of the angle of observation. The channel centroid values fitted by a least-squares technique, yielded experimental attenuation factors, F. The stopping theories of Lindhard *et al* (1963) and Blaugrund (1966) were used to find the theoretical attenuation factors and the corresponding mean lifetimes, τ_m. The empirical normalization constants, f_e and f_n, were taken to be unity. The range of ^{37}Ar ions in CdS, approximately 400 $\mu g\,cm^{-2}$, was 40% of the target thickness. Experimentally, the ^{37}Ar nuclei could have been created at any depth in the CdS target. In the computations for each bombarding energy the target was artificially divided into ten 100 $\mu g\,cm^{-2}$ layers to account for this situation. Calculations were made for each layer assuming that the ^{37}Ar nuclei were formed at the centre and stopped in the remainder of the target. The gold backing was included for the rear layers where the range of the ^{37}Ar ions was greater than the residual CdS. The ten theoretical attenuation factor against mean lifetime, F–τ_m, curves were averaged to give the final curve which was used to determine the lifetimes. Figure 3 displays two F–τ_m curves. Curve A was computed as described above. Curve B was calculated assuming that the ^{37}Ar nuclei were made in the middle of the 1·0 mg cm^{-2} CdS target and that no stopping occurred in the gold backing.

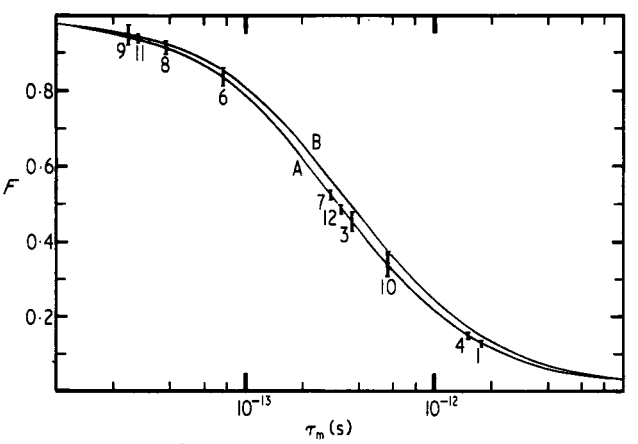

Figure 3. Two curves of F plotted against τ_m calculated for ^{37}Ar ions in $Cd^{34}S$ at an alpha energy of 9·0 MeV. Curve A included the effects of stopping in the gold backing as described in the text. Curve B was calcuated by assuming that the ^{37}Ar ions were formed at the centre of the target with no stopping in the gold. Curve A was used to assign lifetime values. The numbers under the experimental F values are the level numbers listed in table 1.

Twelve of the eighteen observed Döppler shifts are shown in figure 4. The attenuation factors and resulting mean lifetimes are given in table 1. These τ_m values are compared with previous measurements in table 2.

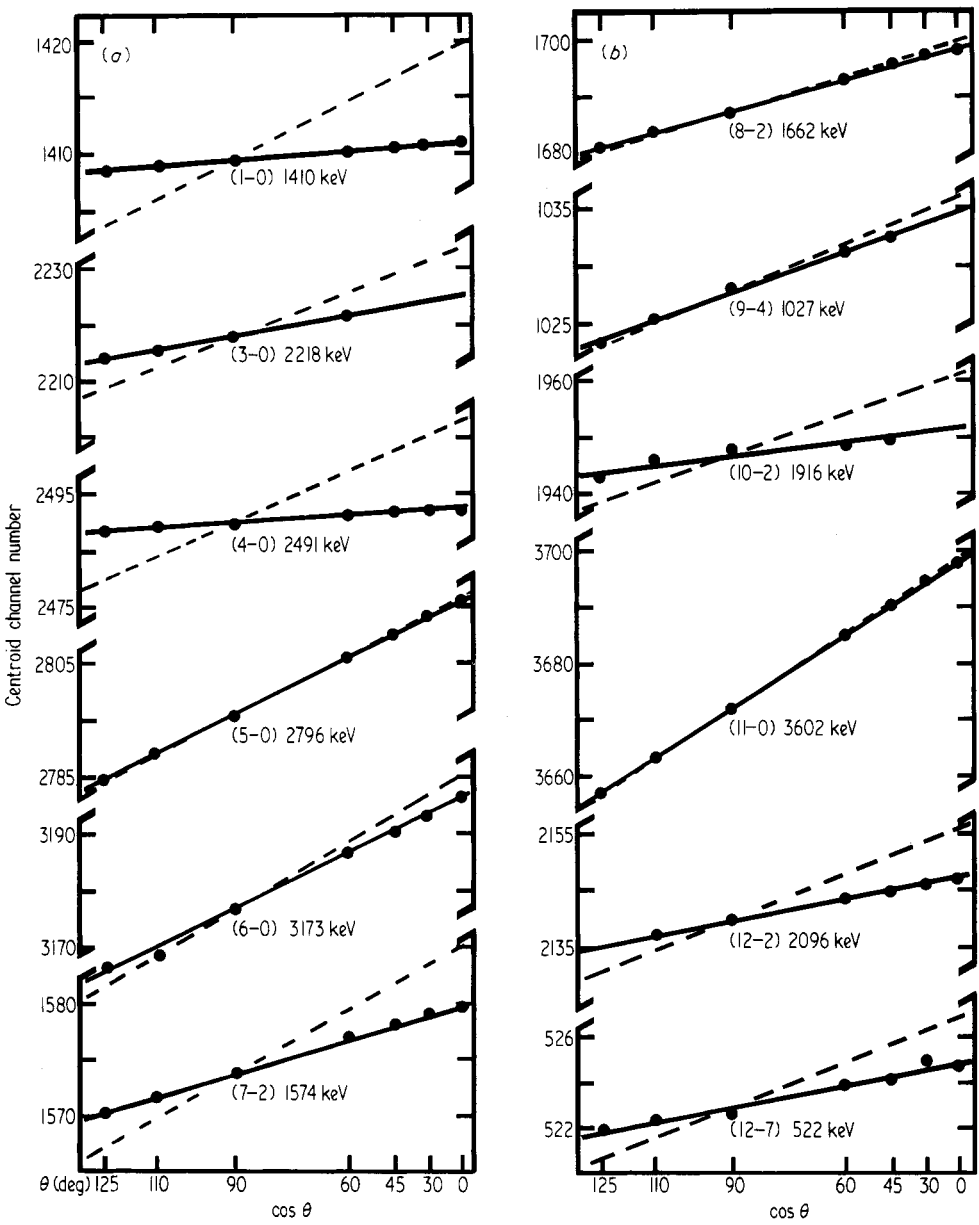

Figure 4. Plots of peak centroid channel against cos θ for twelve of the eighteen γ rays from which DSAM lifetimes were obtained. The energies and corresponding transitions are shown. The full lines are least-squares fits to the data. The full shifts ($F = 1$) are shown as broken lines. The beam energies used were (*a*) 9·0 MeV, and (*b*) 9·5 MeV. The dispersions were 1·00 keV per channel and 0·98 keV per channel, respectively.

3.2. RDM lifetime

The mean lifetime of the 1611 keV level was measured by the RDM at a bombarding energy of 9·0 MeV using eleven target–stopper distances between 1·25 mm and 17·25 mm.

Table 1. Measured energies, attenuation factors, and mean lifetimes

Level	E_x (keV)	E_γ (keV)	E_α (MeV)	F†	τ_m (fs ± 25 %)‡
1	1409·8 ± 0·2	1409·8 ± 0·3	9·0	0·138 ± 0·003	1750 ± 50
		1409·9 ± 0·3	9·5	0·129 ± 0·006§	
2	1611·2 ± 0·2	1611·2 ± 0·3	9·0	0·009 ± 0·009	> 15000
		1611·2 ± 0·3	9·5	not measured	
3	2217·6 ± 0·3	2217·4 ± 0·4	9·0	0·422 ± 0·016	400 ± 25
				0·396 ± 0·034^D	
		2217·9 ± 0·4	9·5	0·466 ± 0·015	
				0·407 ± 0·040^D	
4	2490·7 ± 0·2	2490·1 ± 0·5	9·0	0·138 ± 0·008§	1620 ± 100
		2490·4 ± 0·5	9·5	0·150 ± 0·011§	
		879·5 ± 0·2	9·0	0·153 ± 0·015§	
		880·0 ± 0·2	9·5	‖	
5	2796·4 ± 0·4	2796·2 ± 0·6	9·0	0·989 ± 0·004	< 15
				1·007 ± 0·008^D	
		2796·6 ± 0·6	9·5	0·974 ± 0·009§	
				0·983 ± 0·006§^{D}	
6	3172·6 ± 0·7	3172·6 ± 0·7	9·0	0·834 ± 0·022	75 ± 10
7	3185·2 ± 0·3	1574·0 ± 0·3	9·0	0·537 ± 0·006	280 ± 10
		1574·0 ± 0·3	9·5	0·521 ± 0·012§	
8	3273·9 ± 0·2	3273·8 ± 0·7	9·0	0·939 ± 0·005	35 ± 5
		3273·6 ± 0·7	9·5	0·927 ± 0·010§	
				0·943 ± 0·019§^{D}	
		1661·8 ± 0·3	9·0	0·914 ± 0·010	
		1661·8 ± 0·3	9·5	0·883 ± 0·012§	
		784·0 ± 0·2	9·0	0·934 ± 0·018	
		783·6 ± 0·2	9·5	0·907 ± 0·022	
9	3518·3 ± 0·3	2108·9 ± 0·4	9·5	‖	25 ± 15
		1027·2 ± 0·3	9·5	0·943 ± 0·030	
10	3527·2 ± 0·2	1916·5 ± 0·4	9·5	0·322 ± 0·019	590 ± 80
		730·5 ± 0·2	9·5	0·321 ± 0·019	
		342·3 ± 0·2	9·5	0·350 ± 0·028	
		253·1 ± 0·2	9·5	0·382 ± 0·100	
11	3601·8 ± 0·8	3601·8 ± 0·8	9·5	0·938 ± 0·005	30 ± 5
				0·928 ± 0·020^D	
12	3707·3 ± 0·4	2096·4 ± 0·4	9·5	0·478 ± 0·010	370 ± 20
		521·8 ± 0·2	9·5	0·497 ± 0·048	

† The attenuation factor was usually obtained from the escape-suppressed data. A superscript D indicates that the value was obtained from the pair-escape data.

‡ A 25 % error is shown in the time scale as an indication of the uncertainties in the stopping theory.

§ The attenuation factor was corrected for feeding from higher levels.

‖ The F value could not be measured due to the interference of other γ rays at angles other than 90°.

The mean recoil velocity was $\beta = 0{\cdot}617 \pm 0{\cdot}012\,\%$. After corrections for velocity spread (2 %), solid angle (10 %), and detector efficiency (0·1 %), the mean distance was found to be $11{\cdot}24 \pm 0{\cdot}49$ mm corresponding to $\tau_m = 6{\cdot}08 \pm 0{\cdot}28$ ns. The decay curve is shown in figure 5. This result is compared with previous measurements in table 2. The agreement is remarkable in the case of Ragan *et al* (1971a) because the experimental parameters were quite different for the two measurements.

Table 2. Comparison of present and previous mean lifetime measurements

	DSAM τ_m(fs)						
E_x (keV)	Present work $^{34}S(\alpha, n\gamma)^{37}Ar$	Ragan *et al* (1971b) $^{34}S(\alpha, n\gamma)^{37}Ar$	Kruzek *et al* (1973) $^{37}Cl(p, n\gamma)^{37}Ar$	Luketina *et al* (1972) $^{37}Cl(p, n\gamma)^{37}Ar$	Wong *et al* (1972) $^{37}Cl(p, n\gamma)^{37}Ar$	Caraca *et al* (1971) $^{37}Cl(p, n\gamma)^{37}Ar$	Ivascu *et al* (1971) $^{35}Cl(\tau, p\gamma)^{37}Ar$
1410	1750 ± 50	1080^{+170}_{-130}	620 ± 185	1220 ± 150	943 ± 35	370^{+190}_{-110}	650 ± 350
2218	400 ± 25	3804 ± 50	540 ± 145	910 ± 190	510 ± 67		600 ± 180
2491	1620 ± 100	775^{+105}_{-90}	775 ± 170	1040 ± 140	660 ± 205	88 ± 24	400 ± 130
2796	< 15	14 ± 11	23 ± 8	< 40	22 ± 14	< 8	< 25
3173	75 ± 10		81 ± 15	100 ± 20			30 ± 15
3185	280 ± 10		310 ± 80	300 ± 40	285 ± 62		950 ± 450
3274	35 ± 5		38 ± 15	60 ± 20	50 ± 18		45 ± 30
3518	25 ± 15		93 ± 35	< 40			220 ± 120
3527	590 ± 80		> 1200	600 ± 300			
3602	30 ± 5		82 ± 25	< 60			50 ± 15

	RDM τ_m(ns)				
E_x (keV)	Present work $^{34}S(\alpha, n\gamma)^{37}Ar$ eleven distances	Verucchi *et al* (1973) $^{34}S(\alpha, n\gamma)^{37}Ar$ fourteen distances	Ragan *et al* (1971a) $^{34}S(\alpha, n\gamma)^{37}Ar$ eight distances	Goosman and Kavanagh (1967) $^{34}S(\alpha, n\gamma)^{37}Ar$ one distance	Randolph *et al* (1971) $^{37}Cl(p, n\gamma)^{37}Ar$ magnetic moment measurement
1611	$6{\cdot}08 \pm 0{\cdot}28$	$6{\cdot}47 \pm 0{\cdot}22$	$6{\cdot}08 \pm 0{\cdot}29$	$7{\cdot}4 \pm 0{\cdot}7$	$6{\cdot}6 \pm 0{\cdot}2$

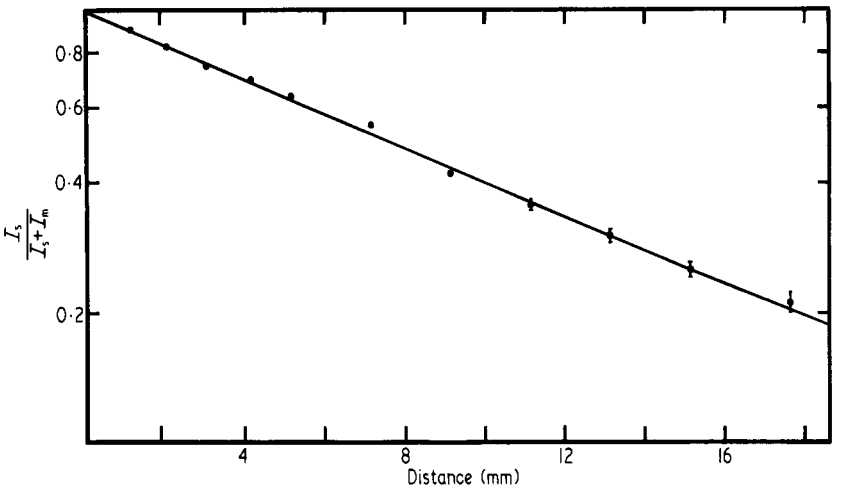

Figure 5. Recoil distance method decay curve for the 1611 keV γ ray. The mean lifetime of the 1611 keV level was determmed to be $6{\cdot}08 \pm 0{\cdot}28$ ns. The full line is a least-squares fit to the experimental data. I_s and I_m are the intensities of the stationary and moving γ ray decays, respectively. $V/c = 0{\cdot}617 \pm 0{\cdot}012\,\%$ and $D_M = 11{\cdot}24 \pm 0{\cdot}49$ mm.

3.3. Angular correlations and linear polarizations

The angular correlations of fifteen gamma transitions were obtained at bombarding energies of 9·0 MeV and 9·5 MeV by measuring their intensities at five angles, 90°. 60°, 45°, 30° and 0°. Normalization was accomplished using the isotropic 1410 keV $\frac{1}{2}^+ \rightarrow \frac{3}{2}^+$ transition. Mixing ratios δ and predicted linear polarizations were found by a least-squares fitting analysis of the experimental angular distributions. The sign convention for δ was that of Rose and Brink (1967). Error limits on the mixing ratios were assigned using the method of Cline and Lesser (1970). The values of the relative substate populations used in the fitting procedure were obtained from the statistical model program, MANDY (Sheldon and van Patter 1966), for the incident beam energy. The sensitivity of δ to the population parameters was investigated for several of the strongest γ rays which were studied by using an alternative fitting procedure in which the substate populations were allowed to vary. In all cases the mixing ratio obtained was the same within errors as that found using the MANDY predictions. Usually the best fit to an angular distribution was obtained for a value of the first substate population which was within 5 % of that predicted by MANDY.

Several of the spins and parities of the ^{37}Ar levels studied had not previously been established. Including gamma linear polarization measurements with the angular correlation data has allowed definite assignments to be made. These levels are discussed below. Table 3 gives the measured mixing ratios, the predicted linear polarizations derived from the angular correlation data, the experimental linear polarizations, and, for completeness, the transition strengths. Mixing ratios and branching ratios found by other workers are compared with the present results in table 4 and table 5, respectively.

3.4. Spin and/or parity assignments

3.4.1. The 3173 keV level. The 3173 keV ($6 \rightarrow 0$) transition forms a doublet with the ^{35}Cl 3163 keV ($6 \rightarrow 0$) transition. A gaussian peak fitting routine was used to extract the

Table 3. Measured angular distribution coefficients, mixing ratios, linear polarizations, and transition strengths

E_x (keV)	E_γ (keV)	Legendre coefficients† a_2	a_4	$J_i^\pi \to J_f^\pi$	δ	Polarization Predicted‡	Measured	Multipolarity	Transition strength (Wu) Electric	Magnetic
2796	2796	-0.05 ± 0.02	$+0.01 \pm 0.00$	$\frac{5}{2}^+ \to \frac{3}{2}^+$	-0.16 ± 0.01	-0.57 ± 0.01	-0.45 ± 0.13	E2/M1	> 1.0	> 0.09
3173	3173	-0.95 ± 0.04	$+0.08 \pm 0.04$	$\frac{5}{2}^+ \to \frac{3}{2}^+$	$+0.52 \pm 0.09$	$+0.04 \pm 0.03$	-0.22 ± 0.20	E2/M1	1.0 ± 0.4	$(10 \pm 3) \times 10^{-3}$
3185	1574	$+0.65 \pm 0.01$	$+0.14 \pm 0.01$	$\frac{9}{2}^- \to \frac{7}{2}^-$	-0.64 ± 0.05	-0.91 ± 0.01	-0.80 ± 0.09	E2/M1	12 ± 3	$(21 \pm 5) \times 10^{-3}$
3274	3274	-0.22 ± 0.03	0.00 ± 0.03	$\frac{5}{2}^- \to \frac{3}{2}^+$	-0.07 ± 0.05	$+0.52 \pm 0.03$	$+0.75 \pm 0.29$	M2/E1	$(0.32 \pm 0.07) \times 10^{-3}$	$0.7^{+1.6}_{-0.6}$
	1662	$+0.22 \pm 0.02$	0.00 ± 0.02	$\frac{5}{2}^- \to \frac{7}{2}^-$	$+0.32 \pm 0.07$	-0.36 ± 0.05	-0.44 ± 0.18	E2/M1	11 ± 6	$(85 \pm 22) \times 10^{-3}$
	784	$+0.23 \pm 0.06$	0.00 ± 0.06	$\frac{5}{2}^- \to \frac{3}{2}^-$	-0.06 ± 0.10	-0.49 ± 0.04	-0.44 ± 0.23	M1		0.15 ± 0.03
3527	1916	-0.39 ± 0.03	-0.32 ± 0.04	$\frac{7}{2}^- \to \frac{7}{2}^-$	$+3.5 \pm 1.3$	-0.37 ± 0.05	-0.31 ± 0.31	E2/M1	4.6 ± 1.4	$(0.39^{+0.63}_{-0.22}) \times 10^{-3}$
	731	-0.21 ± 0.09	0.00 ± 0.10	$\frac{7}{2}^- \to \frac{5}{2}^+$	-0.06 ± 0.06	-0.49 ± 0.05	-0.03 ± 0.23	E1	$(0.31 \pm 0.06) \times 10^{-3}$	
	342	-0.01 ± 0.02	0.00 ± 0.03	$\frac{7}{2}^- \to \frac{9}{2}^-$	-0.10 ± 0.14	-0.30 ± 0.10	§	M1		0.28 ± 0.06
	253	-0.28 ± 0.08	0.00 ± 0.11	$\frac{7}{2}^- \to \frac{5}{2}^-$	$+0.03^{+1.02}_{-0.17}$	-0.45 ± 0.15	§	M1		0.13 ± 0.03
3602	3602	$+0.03 \pm 0.03$	-0.09 ± 0.03	$\frac{3}{2}^+ \to \frac{3}{2}^+$	$+0.24 \pm 0.08$	$+0.51 \pm 0.01$	$+0.96 \pm 0.45$	E2/M1	$0.33^{+0.35}_{-0.22}$	$(21 \pm 5) \times 10^{-3}$
				$\frac{5}{2}^- \to \frac{3}{2}^+$	-0.19 ± 0.05	$+0.63 \pm 0.04$		M2/E1	$(0.61 \pm 0.15) \times 10^{-3}$	8^{+7}_{-4}
3707	2096	$+0.37 \pm 0.02$	-0.29 ± 0.02	$\frac{7}{2}^- \to \frac{7}{2}^-$	-1.40 ± 0.09	-0.49 ± 0.04	$+1.02 \pm 0.28$	E2/M1	4.2 ± 1.0	$(2.7 \pm 0.7) \times 10^{-3}$
				$\frac{11}{2}^- \to \frac{7}{2}^-$ ‖	$+0.04 \pm 0.04$	$+0.69 \pm 0.04$		E2	6.3 ± 1.3	
	522	-0.29 ± 0.06	0.00 ± 0.06	$\frac{7}{2}^- \to \frac{9}{2}^-$	-0.11 ± 0.07	-0.13 ± 0.05	-0.37 ± 0.25	E2/M1	15^{+28}_{-13}	$(89 \pm 20) \times 10^{-3}$
				$\frac{11}{2}^- \to \frac{9}{2}^-$ ‖	$+0.01 \pm 0.05$	-0.41 ± 0.04		M1		$(91 \pm 19) \times 10^{-3}$

† Normalized to $a_0 = 1$ and corrected for solid angle effects.

‡ The sign of the predicted polarization corresponds to the parity indicated for the initial spin value. Changing the parity changes the sign.

§ The polarimeter had an energy cut off of about 450 keV.

‖ This $\frac{11}{2}$ spin is selected by the polarization data as the predicted polarization for the $\frac{7}{2}$ possibility is more than three standard deviations from the experimental polarization.

Table 4. Comparison of present and previous mixing ratio measurements

E_x (keV)	E_γ (keV)	Present work	Alenius *et al* (1972)	Wong *et al* (1972)	Taras *et al* (1972)	Champlin *et al* (1971)
2796	2796	-0.16 ± 0.01		-0.21 ± 0.13	-0.16 ± 0.03	0.00 ± 0.15
3173	3173	$+0.52 \pm 0.09$		$+0.7 \pm 1.0$		$+0.3 \pm 0.3$
3185	1574	-0.64 ± 0.05	$-4.7^{+1.4}_{-3.4}$	-0.58 ± 0.09		
3274	3274	-0.07 ± 0.05		-0.03 ± 0.13		
3527	1916	$+3.5 \pm 1.3$	$+2.1^{+5.0}_{-0.7}$			$\leqslant -25$ or $\geqslant +1.0$
3602	3602	$+0.24 \pm 0.08(\frac{3}{2}^+)$				
		$-0.19 \pm 0.05(\frac{5}{2}^-)$				-0.28 ± 0.03
3707	2096	$+0.04 \pm 0.04$	0.1 ± 0.1			

experimental angular distribution. The fitting analysis of this distribution gave a unique spin assignment of $\frac{5}{2}$. This confirms the results of Wong *et al* (1972). The mixing ratio combined with the mean lifetime measurement rules out negative parity since this would give an M2 ground state transition strength of greater than 20 Wu (Weisskopf single particle units). Thus, $J^\pi = \frac{5}{2}^+$ for this level.

3.4.2. The 3274 keV level. Analysis of the 3274 keV and 1662 keV γ-ray angular distributions gives spins of $\frac{3}{2}$ or $\frac{5}{2}$. The $\frac{3}{2}$ possibility may be eliminated by transition strength arguments in agreement with the work of Ivascu *et al* (1971). The polarization data in table 3 for the 3274 keV and 1662 keV γ rays show that the parity is negative. The assignment is $J^\pi = \frac{5}{2}^-$ for this level.

3.4.3. The 3527 keV level. Fitting the angular distributions of the four gamma transitions from this level results in a spin of $\frac{7}{2}$, as was also shown by Champlin *et al* (1971). Our mean lifetime and mixing ratio measurements give an unacceptable M2 strength of greater than 130 Wu for the 1916 keV γ ray assuming positive parity. Therefore, $J^\pi = \frac{7}{2}^-$ for this level.

3.4.4. The 3602 keV level. The angular distribution of the 3602 keV γ ray gives acceptable fits for both $\frac{3}{2}$ and $\frac{5}{2}$ spins which agrees with the work of Champlin *et al* (1971). The polarization results shown in table 3 give positive and negative parity for the $\frac{3}{2}$ and $\frac{5}{2}$ possibilities, respectively. Sen *et al* (1971) assigned $J^\pi = \frac{3}{2}^-$ on the basis of weakly excited $l = 1$ momentum transfer in the ^{36}Ar(d, p)^{37}Ar reaction. This assignment is questionable as Mermaz *et al* (1971) using the same reaction were unable to reproduce the results of Sen *et al* (1971) for several weakly excited states. We find the spin and parity possibilities of $J^\pi = \frac{3}{2}^+$ or $J^\pi = \frac{5}{2}^-$ for this level.

3.4.5. The 3707 keV level. The angular correlation data shown in figure 6 gave spin possibilities of $\frac{7}{2}$ or $\frac{11}{2}$. The transition strengths obtained by combining the δ and τ_m data required the parity to be negative. The polarization results of table 3 show that the parity must be positive for the spin $\frac{7}{2}$ possibility. Confirming the suggestion of Alenius *et al* (1972), we find $J^\pi = \frac{11}{2}^-$ for this level.

Table 5. Comparison of present and previous branching ratio measurements

E_x (keV)	E_γ (keV)	Present work	Alenius *et al* (1972)	Luketina *et al* (1972)	Wong *et al* (1972)	Caraca *et al* (1971)	Champlin *et al* (1971)	Ivascu *et al* (1971)
2491	2491	93·0 ± 0·5		91 ± 2	95 ± 3	88 ± 3	91 ± 2	100
	880	7·0 ± 0·5		9 ± 2	5 ± 3	12 ± 3	9 ± 2	
3274	3274	45 ± 2	50	56 ± 5	43 ± 2	45 ± 6	60 ± 5	39 ± 7
	1662	47 ± 2	50	38 ± 5	57 ± 2	55 ± 6	40 ± 5	55 ± 8
	784	8 ± 1						
	477	†		6 ± 3				6 ± 3
3518	2109	90‡		69 ± 4		100	74 ± 3	93 ± 4
	1027	10‡		24 ± 4			26 ± 6	
	344		§	7 ± 4				7 ± 4
3527	1916	67 ± 1	76	100		100	100	100
	731	8 ± 1						
	342	21 ± 2	24					
	253	4·0 ± 0·5						
3707	2096	85 ± 1	86					
	522	15 ± 1	14					

† An unidentified γ ray of this energy was observed at bombarding energies below the threshold of the 3274 keV level.

‡ Estimates based on the 90° data due to contamination of 2109 keV γ ray. The values given by Champlin *et al* (1971) are quoted in figure 1.

§ The γ–γ coincidence data showed that this γ ray was associated with the 3527 keV evel.

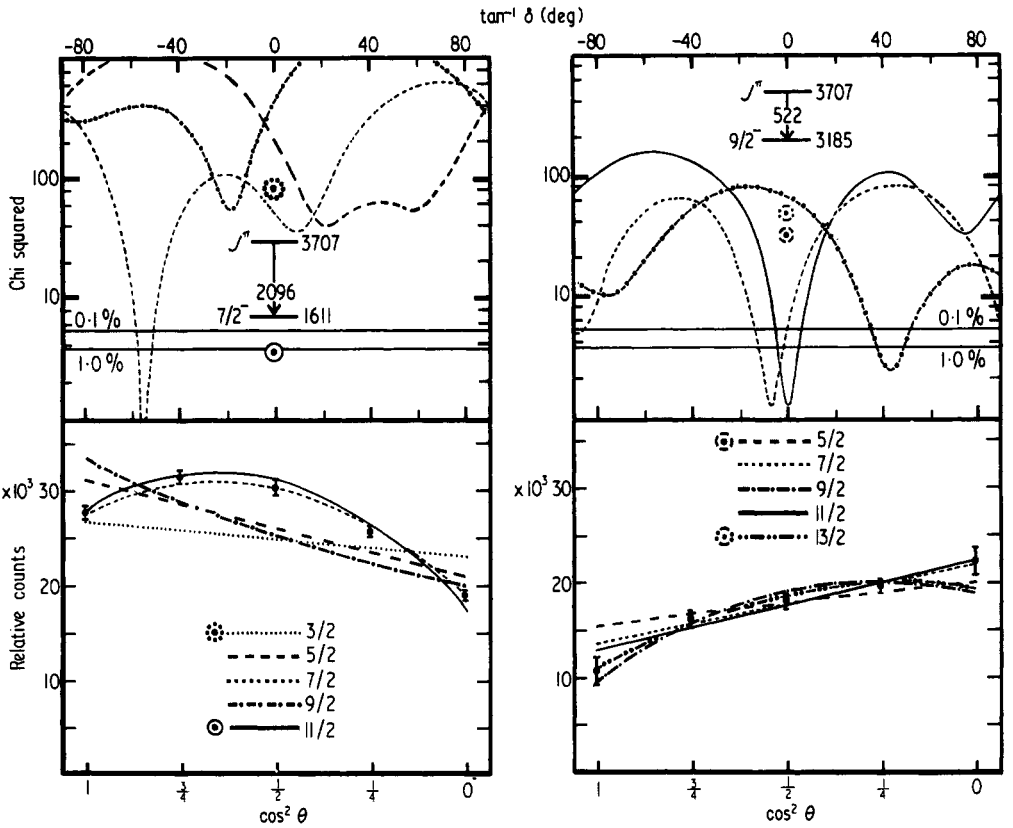

Figure 6. Experimental angular distributions and chi-squared against $\tan^{-1}$ plots for the 2096 keV and 522 keV gamma transitions from the 3707 keV level. The results of the fits for the various spin possibiities are shown together with the 1·0 % and 0·1 % confidence limits.

4. Discussion

4.1. Positive parity levels

Calculations in the full space of s–d shell model wavefunctions for positive parity states of nuclei with $A = 34$–38 have been made by Wildenthal *et al* (1971). In figure 7 the experimental positive parity levels are compared with two calculations (Wildenthal *et al* 1971) using different interactions. The agreement for the first four states is fairly good, but the $\frac{3}{2}^+$ excited state lies about 1·0 MeV higher in the model than the probable experimental $\frac{3}{2}^+$ level. Table 6 compares the experimentally observed E2 and M1 transition strengths with the calculated values (Wildenthal *et al* 1971). The agreement is good for the electric strengths, but only fair for the magnetic strengths.

It has been observed in stripping reactions (Mermaz *et al* 1971, Sen *et al* 1971, Endt and van der Leun 1967) that low-lying levels in ^{37}Ar have large fractions of the single particle widths for adding a $1f_{7/2}$ or a $2p_{3/2}$ neutron to ^{36}Ar. States of this nature occur in ^{37}Ar at excitations of 1611 keV, 2491 keV, and 3518 keV. Configurations of even numbers of particles in the f–p shell are thus likely to occur at excitation energies of about 4·0 MeV. Better agreement with experiment should be obtained in calculations which allow f–p shell states to mix with s–d shell states.

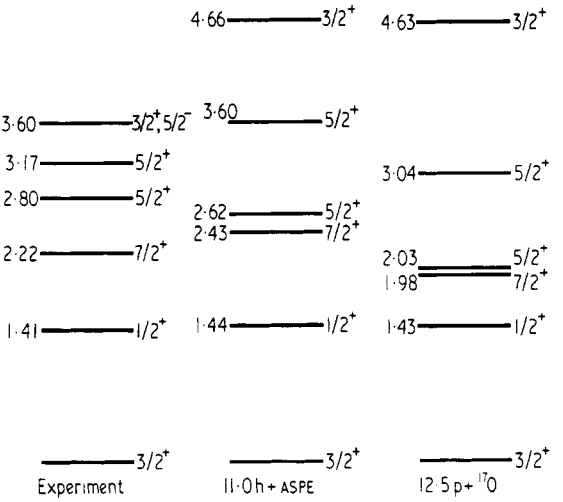

Figure 7. Comparison of the experimental ^{37}Ar positive parity states with those predicted by the shell model calculations of Wildenthal *et al* (1971) using two different interactions. The level energies are given in MeV.

4.2. Negative parity levels

A core excitation model has been developed by de Shalit (1961) in which an odd-mass nucleus is formed by adding a single nucleon to an even–even core nucleus. If the odd particle is weakly coupled to the core, the spectrum of excited states might consist of excited states of the core as well as excitations of the odd nucleon. We present evidence which shows that the low-lying negative parity levels of ^{37}Ar may be described in terms of this model.

Stripping reactions have shown that most of the $1f_{7/2}$ single particle strength may be identified with the $\frac{7}{2}^-$ level at 1611 keV (Endt and van der Leun 1967). This level is taken to be the 'ground' state in the core excitation description. A neutron in the f–p shell would not be expected to greatly influence the core nucleus, ^{36}Ar. The low-lying excited states of ^{36}Ar exhibit an apparently good nuclear vibrational spectrum (Endt and van der Leun 1967). We assume that the excited ^{36}Ar core is the 2^+ level at 1970 keV. Coupling a spin $\frac{7}{2}$ particle to a spin 2 core produces a quintet of states with spins ranging from $\frac{3}{2}$ to $\frac{11}{2}$. Five states with these spins are observed to decay to the 1611 keV 'ground' state as shown in figure 8. If the weak coupling approximation is valid, the 'centre of gravity' of this multiplet should coincide with the corresponding state of the unperturbed core nucleus. Figure 8 shows that the 'centre of gravity' of the ^{37}Ar quintet is about 10% lower than the 2^+ level of ^{36}Ar.

The core excitation model makes two predictions concerning the E2 transition strengths between the multiplet and the 'ground' state. First, each transition should have the same E2 strength. Second, this value should be the same as that for the corresponding transition in the core nucleus. It may be seen from the data shown in figure 8 that these criteria are reasonably well satisfied.

A further test is provided by the M1 transition strengths within the multiplet. In the core excitation model these are given by the following expression:

$$B(\mathrm{M1}) = (2J_\mathrm{f}+1)j_\mathrm{p}(j_\mathrm{p}+1)(2j_\mathrm{p}+1)\begin{Bmatrix} J_\mathrm{i} & J_\mathrm{f} & 1 \\ j_\mathrm{p} & j_\mathrm{p} & j_\mathrm{c} \end{Bmatrix}^2 (g_\mathrm{c}-g_\mathrm{p})^2$$

Table 6. Comparison of measured and calculated transition strengths for positive parity states

		E2 Strength (Wu)			M1 Strength (Wu × 10^{-3})		
E_x (keV)	$J_i^\pi \rightarrow J_f^\pi$	Experiment	Interaction (11·0h + ASPE†)	Interaction (12·5p + ^{17}O†)	Experiment	Interaction (11·0h + ASPE†)	Interaction (12·5p + ^{17}O†)
1410	$\frac{1}{2}^+ \rightarrow \frac{3}{2}^+$	12·0 + 0·4‡	9·3	8·5	7 ± 2‡	19	20
2218	$\frac{7}{2}^+ \rightarrow \frac{3}{2}^+$	5·2 ± 0·4	5·1	4·7			
2796	$\frac{5}{2}^+ \rightarrow \frac{3}{2}^+$	> 1·0	2·9	2·7	> 90	430	490
3173	$\frac{5}{2}^+ \rightarrow \frac{3}{2}^+$	1·0 ± 0·4	0·60	0·93	10 ± 3	52	58
3602	$\frac{3}{2}^+ \rightarrow \frac{3}{2}^+$	$0{\cdot}33^{+0{\cdot}35}_{-0{\cdot}22}$	0·30	0·30	21 ± 5	34	48

† This refers to the interaction used by Wildenthal *et al* (1971) in their shell model calculations.
‡ The mixing ratio undetermined. The pure value was calculated.

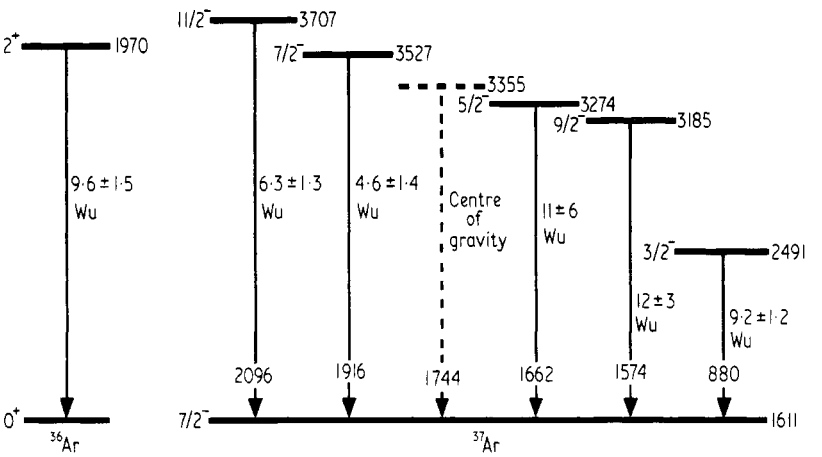

Figure 8. Comparison of the E2 transition strength of the first excited state of ^{36}Ar with the E2 strengths of the quintet of negative parity levels which are postulated to result from weakly coupling a $1f_{7/2}$ neutron to a ^{36}Ar core.

where i and f refer to the initial and final spins, c and p refer to the core and particle, the curly brackets represent the 6-*j* symbol of angular momentum coupling and the *g* factor is related to the spin and magnetic moment of the state by $\mu = jg$. Thus, within a multiplet, the ratios of M1 strengths are independent of the values of the core and particle *g* factors. Plotting the M1 strengths against the geometrical factors, as in figure 9, will result in a linear relationship if the core excitation description is valid. The full line in figure 9 is a linear least-squares fit to the data constrained to pass through the origin.

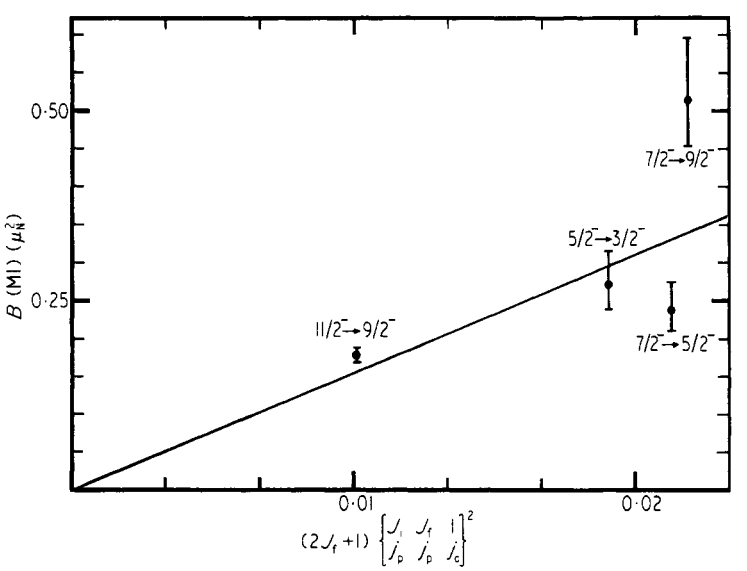

Figure 9. Plot of experimental M1 strengths against geometrical factor for transitions within the quintet of negative parity levels postulated to result from weakly coupling a $1f_{7/2}$ particle to a ^{36}Ar core. The experimental points are labelled with the initial and final spins. The full line is a least-squares fit to the data and its slope is proportional to the square of the difference of the core and particle *g* factors ($(g_c - g_p)^2 = 0{\cdot}54 \pm 0{\cdot}09$).

From the slope of the linear fit the value, $(g_c - g_p)^2 = 0{\cdot}54 \pm 0{\cdot}09$, is found. Since the magnetic moment of the 1611 keV state in ^{37}Ar has been measured to be

$$\mu_p = (-1{\cdot}33 \pm 0{\cdot}05)\mu_N$$

(Randolph *et al* 1971) the magnetic moment of the 1970 keV state in ^{36}Ar may be predicted. The value obtained is $\mu_c = (0{\cdot}70 \pm 0{\cdot}06)\mu_N$. This quantity has not been measured, but a recent shell model calculation (Strottman, private communication) for the first 2^+ state of ^{36}Ar gives $\mu_{2_1}^+ = 1{\cdot}0\,\mu_N$. This is probably an overestimate because other shell model calculations in this mass region (Wildenthal *et al* 1971) give results which are at least 20% larger than the experimental measurements.

Clearly, this application of the core excitation model to ^{37}Ar provides only an approximate description of the structure of the low-lying negative parity states. The 'centre of gravity' of the quintet is about 0·23 MeV lower than the first excited state of ^{36}Ar. This indicates that the coupling between particle and core is stronger than the model assumes. The model does not account for the $\frac{3}{2}^-$ level at 3518 keV. Stripping reactions (Endt and van der Leun 1967) have shown that the single particle $2p_{3/2}$ strength is split about equally between this level and the $\frac{3}{2}^-$ level at 2491 keV which was taken as the lowest member of the quintet. Therefore, the single particle states and the core excitation states are mixed. The two $\frac{7}{2}^-$ states are probably mixed as well.

6. Conclusion

A detailed investigation of the first twelve excited states of ^{37}Ar has been completed. The properties of the positive parity levels are fairly well reproduced by recent shell model calculations. The structure of the negative parity levels may be described qualitatively by the core excitation model. Experiments have been performed and are currently being analysed to determine the characteristics of levels up to 7·1 MeV excitation in ^{37}Ar. Calculations using the unified vibrational model are also being performed in an attempt to gain a better understanding of the structure of the negative parity levels.

Acknowledgments

This work was supported by grants from the United Kingdom Science Research Council. Two of us (PJN and DAV) were the recipients of SRC Postgraduate Studentships.

References

Alenius N G, Skeppstedt O and Wallander E 1972 *Phys. Scr.* **6** 296–302
Blaugrund A E 1966 *Nucl. Phys.* **88** 501–12
Butler P A *et al* 1973 *Nucl. Instrum. Meth.* **108** 497–502
Camp D C and Meredith G L 1971 *Nucl. Phys.* A **166** 349–77
Caraca J M G, Gill R D, Johnson P B and Rose H J 1971 *Nucl. Phys.* A **176** 273–83
Champlin J W, Howard A J and Olness J W 1971 *Nucl. Phys.* A **164** 307–20
Cline D and Lesser P M S 1970 *Nucl. Instrum. Meth.* **82** 291–3
de Shalit A 1961 *Phys. Rev.* **122** 1530–6
Endt P M and van der Leun C 1967 *Nucl. Phys.* A **105** 265–70
Goosman D R and Kavanagh R W 1967 *Phys. Lett.* **24B** 507–9

Hardell R and Beer C 1970 *Phys. Scr.* **1** 85–8
Ivascu M, Popescu D and van Middelkoop G 1971 *Nucl. Phys.* A **163** 418–24
Kruzek R G, Chenevert G M, Leighton H G and Kern B D 1973 *Nucl. Phys.* A **202** 530–4
Lindhard J, Scharff M and Schiott H E 1963 *K. danske Vidensk. Selsk., Math.-fys. Meddr* **33** No 14
Luketina I A, Brock J E and Poletti A R 1972 *Phys. Rev.* C **6** 196–204
Mermaz M C *et al* 1971 *Phys. Rev.* C **4** 1778–800
Nolan P J *et al* 1973 *J. Phys.* A: *Math., Nucl. Gen.* **6** L37–40
Ragan C E III *et al* 1971a *Phys. Rev.* C **3** 2076–8
—— 1971b *Phys. Rev.* C **3** 1152–61
Randolph W L Jr *et al* 1971 *Phys. Rev. Lett.* **27** 603–6
Rose H J and Brink D M 1967 *Rev. mod. Phys.* **39** 306–47
Sen S, Hollas C L and Riley P J 1971 *Phys. Rev.* C **3** 2314–22
Sharpey-Schafer J F *et al* 1971 *Nucl. Phys.* A **167** 602–24
Sheldon E and van Patter D M 1966 *Rev. mod. Phys.* **38** 143–86
Skeppstedt O, Hardell R and Arnell S E 1968 *Ark. Fys.* **35** 527–37
Taras P, Turcotte A and Vaillancourt R 1972 *Can. J. Phys.* **50** 1182–94
Taras P, Turcotte A, Vaillancourt R and Matas J 1971 *Can. J. Phys.* **49** 1215–24
Verucchi M J, Vaillancourt R, Cardinal C and Taras P 1973 *Can. J. Phys.* **51** 1039–41
Wildenthal B H, Halbert E C, McGrory J B and Kus T T S 1971 *Phys. Rev.* C **4** 1266–314
Wille P 1968 *Atomkernenergie* **13** 383–4
Wong E *et al* 1972 *Nucl. Phys.* A **192** 279–90